

Throughput Optimal Policies for Energy Harvesting Wireless Transmitters with Non-Ideal Circuit Power

Jie Xu and Rui Zhang

Abstract— Characterizing the fundamental tradeoffs for maximizing energy efficiency (EE) versus spectrum efficiency (SE) is a key problem in wireless communication. In this paper, we address this problem for a point-to-point additive white Gaussian noise (AWGN) channel with the transmitter powered solely via energy harvesting from the environment. In addition, we assume a practical on-off transmitter model with *non-ideal* circuit power, i.e., when the transmitter is on, its consumed power is the sum of the transmit power and a constant circuit power. Under this setup, we study the optimal transmit power allocation to maximize the average throughput over a finite horizon, subject to the time-varying energy constraint and the non-ideal circuit power consumption. First, we consider the *off-line* optimization under the assumption that the energy arrival time and amount are *a priori* known at the transmitter. Although this problem is non-convex due to the non-ideal circuit power, we show an efficient optimal solution that in general corresponds to a *two-phase* transmission: the first phase with an *EE-maximizing* on-off power allocation, and the second phase with a *SE-maximizing* power allocation that is non-decreasing over time, thus revealing an interesting result that both the EE and SE optimizations are unified in an energy harvesting communication system. We then extend the optimal off-line algorithm to the case with multiple parallel AWGN channels, based on the principle of *nested optimization*. Finally, inspired by the off-line optimal solution, we propose a new *online* algorithm under the practical setup with only the past and present energy state information (ESI) known at the transmitter.

Index Terms—Energy harvesting, power control, energy efficiency, spectrum efficiency, circuit power.

I. INTRODUCTION

GREEN or energy efficient wireless communication has recently drawn significant attention due to the growing concerns about the operator's cost as well as the global environmental cost of using fossil fuel based energy to power cellular infrastructures [1], [2], [3]. To achieve the optimal energy usage efficiency for cellular networks, various innovative “green” techniques across different layers of communication protocol stacks have been proposed [4], [5]. Among others, how to maximize the bits-per-Joule *energy efficiency* (EE) for the point-to-point wireless link has received a great deal of interest recently [6], [7], [8].

Besides maximizing EE, another key design objective in wireless communication is to maximize the *spectrum efficiency* (SE) or the number of transmitted bits-per-second-per-Hz (bps/Hz), due to the explosive growth of wireless devices and

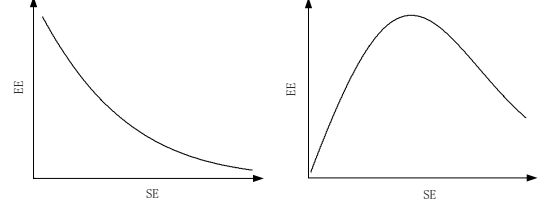


Fig. 1. Tradeoff between EE and SE for the ideal circuit power case of $\alpha = 0$ (the left sub-figure) and the non-ideal circuit power case of $\alpha > 0$ (the right sub-figure).

applications that require high data rates. In order to design wireless communication systems both energy and spectrum efficiently, the fundamental EE-SE relationship needs to be examined carefully. For the simple additive white Gaussian noise (AWGN) channel with bandwidth W and noise power spectral density N_0 , by applying the Shannon's capacity formula, the SE and EE are expressed as $\xi_{SE} = \log_2(1 + \frac{P}{WN_0})$ and $\xi_{EE} = W \log_2(1 + \frac{P}{WN_0})/P$, respectively, with P denoting the transmit power. It thus follows that the optimal EE-SE tradeoff is characterized by $\xi_{EE} = \frac{\xi_{SE}}{(2^{\xi_{SE}} - 1)N_0}$, where ξ_{EE} is a monotonically decreasing function of ξ_{SE} , as shown in the left sub-figure of Fig. 1. In this case, any SE increment will inevitably result in a decrement in EE. However, in practical wireless transmitters, besides the direct transmit power P , there also exists *non-ideal* circuit power consumed when $P > 0$, which accounts for the power consumptions at e.g. the AC/DC converter and the analog radio frequency (RF) amplifier, and amounts to a significant part of the total consumed power at the transmitter. Moreover, when there is no data transmission, i.e., $P = 0$, the transmitter can turn into a *micro-sleep* mode [9], by switching off the power amplifier to reduce the circuit power consumption. For the ease of description, in this paper the transmitter status with $P > 0$ and $P = 0$ are referred to as the *on* and *off* modes, respectively. Denote the non-ideal circuit power during an “on” mode as $\alpha \geq 0$ in Watt, the efficiency of the RF chain as $0 < \eta \leq 1$, and the power consumed during an “off” mode as $\beta \geq 0$ in Watt. A practical power consumption model for the wireless transmitter is given by [10]

$$P_{\text{total}} = \begin{cases} \frac{P}{\eta} + \alpha, & P > 0 \\ \beta, & P = 0, \end{cases} \quad (1)$$

where P_{total} denotes the total power consumed at the transmitter. In practice, β is generally much smaller as compared to α and thus can be ignored for simplicity [5], [7], [8]. In this paper, we assume $\beta = 0$. Therefore, in (1) without loss

J. Xu is with the Department of Electrical and Computer Engineering, National University of Singapore (e-mail: elxjie@nus.edu.sg).

R. Zhang is with the Department of Electrical and Computer Engineering, National University of Singapore (e-mail: elzhang@nus.edu.sg). He is also with the Institute for Infocomm Research, A*STAR, Singapore.

of generality we can further assume $\eta = 1$ since η is only a scaling constant.¹ With the above simplifications, the EE can be re-expressed as $\xi_{EE} = W \log_2(1 + \frac{P}{WN_0})/(P + \alpha)$ for $P > 0$ and the resulting new EE-SE tradeoff is shown in the right sub-figure of Fig. 1 for a given $\alpha > 0$, from which it is observed that the non-ideal circuit power drastically changes the behavior of the EE-SE tradeoff as compared to the ideal case of $\alpha = 0$.

Recently, a new design paradigm for achieving green wireless communication has drawn a great deal of attention, in which wireless terminals are powered primarily or even solely by harvesting the energy from environmental sources such as solar and wind, thereby reducing substantially the energy cost in traditional wireless systems [4], [11]. With the embedded energy harvesting device and rechargeable battery, wireless transmitters can replenish energy from the environment without the need of replacing battery or drawing power from the main grid. Thus, communication utilizing energy harvesting nodes can promisingly achieve a jointly spectrum and energy efficiency maximization goal. However, there are new challenges in designing energy harvesting powered wireless communication, which are not present in traditional systems. For example, the intermittent nature of most practical energy harvesting sources causes random power availability at the transmitter, due to which a new type of transmitter-side power constraint, namely *energy harvesting constraint*, is imposed, i.e., the energy accumulatively consumed up to any time cannot exceed that accumulatively harvested. As a result, existing EE-SE tradeoffs (cf. Fig. 1) revealed for conventional wireless systems assuming a given constant power supply are not directly applicable to an energy harvesting system, with or without the non-ideal circuit power. It is worth noting that some prior work in the literature has investigated the throughput-optimal power control policies for the energy harvesting wireless transmitter assuming an ideal circuit-power model (i.e., $\alpha = 0$, $\eta = 1$, and $\beta = 0$ in (1)), in which useful structural properties of the optimal solution were obtained (see e.g. [12], [13], [14] and references therein). However, there is very limited work on studying the effects of the non-ideal circuit power with $\alpha > 0$ on the throughput-optimal power allocation for energy harvesting communication systems. To our best knowledge, only [15] has proposed a calculus-based approach to address this problem; however, it does not reveal the structure of the optimal solution. Motivated by the known result that the non-ideal circuit power modifies the EE-SE tradeoff considerably in the conventional case with constant power supply as shown in Fig. 1, we expect that it should also play an important role in the EE-SE tradeoff characterization under the new setup with random power supply due to energy harvesting, which motivates our work.

In this paper, we study the throughput maximization problem for a point-to-point AWGN channel with an energy harvesting powered transmitter over a finite horizon. For the purpose of exposition, we assume that the receiver has a constant power supply (e.g. battery). We also assume that at

the transmitter, the renewable energy arrives at a discrete set of time instants with variable energy amount. Under this setup, we investigate the effects of the non-ideal circuit power with $\alpha > 0$ on the throughput-optimal power allocation as well as the resulting new EE-SE tradeoff. The main contributions of this paper are summarized as follows.

- First, we consider the *off-line* optimization under the assumption that the energy arrival time and amount for harvesting are *a priori* known at the transmitter. We show that the optimal power allocation to maximize the average throughput under this setup is a *non-convex* optimization problem, due to the non-ideal circuit power. Nevertheless, we derive an efficient optimal solution for this problem, which is shown to correspond to a novel *two-phase* transmission structure: the first phase with an *EE-maximizing* on-off power allocation, and the second phase with a *SE-maximizing* power allocation that is non-decreasing over time. Thus, we reveal an interesting result that both the EE and SE optimizations are unified in an energy harvesting powered wireless system.
- We then extend the optimal off-line policy for the single-channel case to the general case with multiple parallel AWGN channels, subject to a total energy harvesting power constraint. Using tools from *nested optimization*, we transform this problem with multi-dimensional (vector) power optimization to an equivalent one with only one-dimensional (scalar) power optimization, which can then be efficiently solved by the algorithm derived for the single-channel case.
- Furthermore, inspired by the off-line optimal solution, we propose a heuristic *online* algorithm under the practical setup where only the causal (past and present) energy state information (ESI) for harvesting is assumed to be known at the transmitter. It is shown by simulations that the proposed online algorithm achieves a small performance gap from the throughput upper bound by the optimal off-line solution, and also outperforms other heuristically designed online algorithms.

The rest of this paper is organized as follows. Section II introduces the system model and presents the problem formulation. Section III derives the optimal off-line power allocation policy for the single-channel case. Section IV extends the result to the multi-channel case based on the nested optimization. Section V presents the proposed online algorithm and Section VI evaluates its throughput performance by simulations. Finally, Section VII concludes the paper.

II. SYSTEM MODEL AND PROBLEM FORMULATION

In this paper, we consider the point-to-point transmission over an AWGN channel with constant channel and coherent detection at the receiver. The transmitter is assumed to replenish energy from an energy harvesting device that collects energy over time from a renewable source (e.g. solar or wind). We consider the block-based energy scheduling with each block spanning over T seconds (secs). We assume that the renewable energy arrives during each block at $N - 1$ time instants given by $0 < t_1 < \dots < t_{N-1} < T$, and the

¹Note that the results of this paper can be readily extended to the case with $\eta < 1$ by appropriately scaling the obtained solutions.

energy values collected at these time instants are denoted by E_1, \dots, E_{N-1} , respectively. In general, $N \geq 1$, t_i , and $E_i > 0$, $i = 1, \dots, N-1$, are modeled by an appropriate random process for the given energy source. For convenience, we assume $t_0 = 0$ and denote E_0 as the initial energy stored in the energy storage device at the beginning time of each block. For the purpose of exposition, we assume that the energy storage device has an infinite capacity in this paper. Moreover, we refer to the time interval between two consecutive energy arrivals as an *epoch*, and denote the length of the i th epoch as $L_i = t_i - t_{i-1}$, $i = 1, \dots, N$; for convenience, we denote $t_N = T$.

Suppose that the transmit power over time in each block is denoted by $P(t) \geq 0$, $t \in (0, T]$. Assume that the maximum transmission rate that can be reliably decoded at the receiver at any time t is a function of $P(t)$, given by $C(t) = R(P(t))$, which satisfies the following properties:

- 1) $R(P(t)) \geq 0$, $\forall P(t) \geq 0$, and $R(0) = 0$;
- 2) $R(P(t))$ is a strictly concave function over $P(t) \geq 0$;
- 3) $R(P(t))$ is a monotonically increasing function over $P(t) \geq 0$.

For example, if adaptive modulation and coding (AMC) is applied at the transmitter, then the achievable rate $C(t)$ is denoted by [16]

$$R(P(t)) = W \log_2 \left(1 + \frac{hP(t)}{\Gamma W N_0} \right) \quad (2)$$

in bits-per-sec (bps), where Γ accounts for the gap from the channel capacity due to a practical coding and modulation scheme used; $h > 0$ denotes the constant channel power gain.

As discussed in Section I, we assume an on-off transmitter power model given in (1) with $\beta = 0$ and $\eta = 1$; thus, we rewrite (1) as

$$P_{\text{total}}(t) = \begin{cases} P(t) + \alpha, & P(t) > 0 \\ 0, & P(t) = 0. \end{cases} \quad (3)$$

Since the accumulatively consumed energy up to any time at the transmitter cannot exceed the energy accumulatively harvested, the energy harvesting constraint on the total consumed power is given by

$$\int_0^{t_i} P_{\text{total}}(t) dt \leq \sum_{j=0}^{i-1} E_j, \quad i = 1, \dots, N. \quad (4)$$

Thus, the throughput maximization problem over a finite horizon T can be formulated as follows.

$$\begin{aligned} \max_{P(t) \geq 0} \quad & \int_0^T R(P(t)) dt \\ \text{s.t.} \quad & \int_0^{t_i} P_{\text{total}}(t) dt \leq \sum_{j=0}^{i-1} E_j, \quad i = 1, \dots, N. \end{aligned} \quad (5)$$

The optimal online solution for the above problem with the causal ESI, i.e., for any given t , only E_i 's with $t_i \leq t$ are known at the transmitter, can be numerically solved by the technique of dynamic programming similar to [13]. However, such a solution is of high computational complexity due to "the curse of dimensionality" for dynamic programming. In addition, the resulting solution will not provide any insight to

the structure of the optimal power allocation for an energy harvesting transmitter. Therefore, in this paper, we take an alternative approach by first solving the off-line optimization for (5), assuming that all the energy arrival time t_i 's and amount E_i 's are *a priori* known at the transmitter in each block transmission, and then based on the structure of the off-line optimal solution, devising online algorithms for the practical setup with only causal ESI known at the transmitter.

For the off-line optimization of (5), it is easy to see that the objective function is concave; however, the constraint is non-convex in general since $P_{\text{total}}(t)$ in (3) is a concave function of $P(t)$ if $\alpha > 0$. As a result, the problem is in general non-convex and thus cannot be solved by standard convex optimization techniques. In the next section, we will propose an efficient solution for this problem by exploiting its special structure.

Remark 2.1: It is worth noting that for the off-line optimization, (5) can be shown to be convex if $\alpha = 0$. In this case, similar problems to (5) have been studied in the literature [12], [13], in which the throughput-optimal power allocation $P(t)$ was shown to follow a non-decreasing piecewise-constant (staircase) function over t . This power allocation can be interpreted as maximizing the SE of the point-to-point AWGN channel subject to the new energy harvesting power constraint. As will be shown later in this paper, the non-ideal circuit power with $\alpha > 0$ will change the optimal power allocation for this problem considerably.

III. OFF-LINE OPTIMIZATION

In this section, we solve the off-line optimization problem in (5) with the non-ideal circuit power, i.e., $\alpha > 0$.

A. Reformulated Problem

First, we give the following lemma.²

Lemma 3.1: During any i th epoch $(t_{i-1}, t_i]$, $i = 1, \dots, N$, the optimal solution for (5) is given by $P(t) = P_i > 0$ for the portion of time $\mathcal{T}_i^{\text{on}} \subseteq (t_{i-1}, t_i]$, and $P(t) = 0$ for the remaining time $\mathcal{T}_i^{\text{off}} \subseteq (t_{i-1}, t_i]$, where $\mathcal{T}_i^{\text{on}} \cap \mathcal{T}_i^{\text{off}} = \emptyset$ and $\mathcal{T}_i^{\text{on}} \cup \mathcal{T}_i^{\text{off}} = (t_{i-1}, t_i]$.

Proof: See Appendix A. ■

According to Lemma 3.1 and by denoting the constant transmit power $P_i > 0$ for the "on" period with length $0 \leq l_i^{\text{on}} \leq L_i$ in the i th epoch, (5) can be reformulated as

$$\begin{aligned} \max_{\{P_i\}, \{l_i^{\text{on}}\}} \quad & \sum_{i=1}^N l_i^{\text{on}} R(P_i) \\ \text{s.t.} \quad & P_i > 0, \quad i = 1, \dots, N \\ & 0 \leq l_i^{\text{on}} \leq L_i, \quad i = 1, \dots, N \\ & \sum_{j=1}^i (P_j + \alpha) l_j^{\text{on}} \leq \sum_{j=0}^{i-1} E_j, \quad i = 1, \dots, N. \end{aligned} \quad (6)$$

However, the above problem is still non-convex due to the coupling between P_i 's and l_i^{on} 's. In the following, we first solve this problem for the special case of $N = 1$ and then generalize the solution to the case with $N \geq 1$.

²We thank the anonymous reviewer who brought our attention to [15], in which an alternative proof for Lemma 3.1 is given based on a calculus approach.

B. Single-Epoch Case with $N = 1$

In the single-epoch case with $N = 1$, the problem in (6) is reduced to

$$\begin{aligned} \max_{l_1^{\text{on}}, P_1} \quad & l_1^{\text{on}} R(P_1) \\ \text{s.t.} \quad & P_1 > 0 \\ & 0 \leq l_1^{\text{on}} \leq T \\ & l_1^{\text{on}}(P_1 + \alpha) \leq E_0. \end{aligned} \quad (7)$$

The solution of the above problem is given in the following proposition.

Proposition 3.1: The optimal solution P_1^* and $l_1^{\text{on}*}$ for (7) is expressed as

$$P_1^* = \max \left(P_{ee}, \frac{E_0}{T} - \alpha \right) \quad (8)$$

$$l_1^{\text{on}*} = \frac{E_0}{P_1^* + \alpha} \quad (9)$$

where P_{ee} is given by

$$P_{ee} = \arg \max_{P_1 > 0} \frac{R(P_1)}{P_1 + \alpha}. \quad (10)$$

Proof: See Appendix B. ■

It is worth noting that P_{ee} given in (10) is the optimal power allocation that maximizes the EE of the AWGN channel under the non-ideal circuit power model as shown in [7]. From Proposition 3.1, it follows that if $P_{ee} > \frac{E_0}{T} - \alpha$, we have $P_1^* = P_{ee}$, $l_1^{\text{on}*} < T$ and $l_1^{\text{off}*} = T - l_1^{\text{on}*} > 0$, which corresponds to an on-off transmission. However, if $P_{ee} \leq \frac{E_0}{T} - \alpha$, we have $P_1^* = \frac{E_0}{T} - \alpha$, $l_1^{\text{on}*} = T$ and $l_1^{\text{off}*} = 0$, which corresponds to a continuous transmission. We will see in the next subsection that the EE-maximizing power allocation P_{ee} plays an important role in the general case with $N \geq 1$. Also note that the right-hand side (RHS) of (10) is a quasi-concave function of P_1 since it is concave-over-linear [17]; thus, P_{ee} can be efficiently obtained by a simple bisection search [17].

C. Multi-Epoch Case with $N \geq 1$

Inspired by the solution for the single-epoch case, we derive the optimal solution for (6) in the general case with $N \geq 1$, as given by the following theorem.

Theorem 3.1: The optimal solution of (6), denoted by $[P_1^*, \dots, P_N^*]$ and $[l_1^{\text{on}*}, \dots, l_N^{\text{on}*}]$, is obtained as follows. Denoting

$$\begin{aligned} i_{ee,0} &= 0, \\ i_{ee,j} &= \min \left\{ i \left| \frac{\sum_{k=i_{ee,j-1}}^{i-1} E_k}{\sum_{k=i_{ee,j-1}+1}^i L_k} - \alpha \leq P_{ee}, \right. \right. \\ &\quad \left. \left. i = i_{ee,j-1} + 1, \dots, N \right\}, j \geq 1, \\ J &= \arg \max_{j \geq 0} i_{ee,j}, \\ i_{ee} &= i_{ee,J}, \end{aligned} \quad (11)$$

the optimal transmit power for epochs $1, \dots, i_{ee}$ is given by

$$P_i^* = P_{ee}, \quad i = 1, \dots, i_{ee} \quad (12)$$

and the optimal on-period $l_i^{\text{on}*}, i = 1, \dots, i_{ee}$, is any set of non-negative values satisfying

$$(P_{ee} + \alpha) \sum_{i=1}^{i_{ee}} l_i^{\text{on}*} = \sum_{i=0}^{i_{ee}-1} E_i \quad (13)$$

$$(P_{ee} + \alpha) \sum_{i=1}^j l_i^{\text{on}*} \leq \sum_{i=0}^{j-1} E_i, \quad j = 1, \dots, i_{ee}. \quad (14)$$

Moreover, for epochs $i_{ee} + 1, \dots, N$, the optimal solution is given by

$$l_i^{\text{on}*} = L_i, \quad i = i_{ee} + 1, \dots, N \quad (15)$$

$$P_i^* = \frac{\sum_{k=n_{i-1}}^{n_i-1} E_k}{\sum_{k=n_{i-1}+1}^{n_i} L_k} - \alpha, \quad i = i_{ee} + 1, \dots, N \quad (16)$$

where

$$\begin{aligned} n_{i_{ee}} &= i_{ee}, \\ n_i &= \arg \min_{j: n_{i-1}+1 \leq j \leq N} \left\{ \frac{\sum_{k=n_{i-1}}^{j-1} E_k}{\sum_{k=n_{i-1}+1}^j L_k} - \alpha \right\}, \\ &\quad i = i_{ee} + 1, \dots, N. \end{aligned} \quad (17)$$

Proof: See Appendix C. ■

It is interesting to take note that the optimal transmission policy given in Theorem 3.1 has a *two-phase* structure, which is explained as follows in more details.

- $0 < t \leq t_{i_{ee}}$: In the first phase, the optimal transmission is an on-off one with a constant power P_{ee} for all the on-periods. Note that P_{ee} is the EE-maximizing power allocation given in (10). Also note that the optimal on-periods $l_i^{\text{on}*}, i = 1, \dots, i_{ee}$, may not be unique provided that they satisfy the conditions given in (13) and (14). Without loss of generality, we assume that in each epoch, the transmitter chooses to be on initially with power P_{ee} provided that its stored energy is not used up, i.e., $l_1^{\text{on}*} = \min(E_0/(P_{ee} + \alpha), L_1)$, $l_2^{\text{on}*} = \min((E_1 + E_0 - (P_{ee} + \alpha)l_1^{\text{on}*})/(P_{ee} + \alpha), L_2)$, and so on.
- $t_{i_{ee}} < t \leq T$: In the second phase, a continuous transmission is optimal. Since $l_i^{\text{on}*} = L_i, i = i_{ee} + 1, \dots, N$, the problem in (6) for $i = i_{ee} + 1, \dots, N$, is reduced to

$$\begin{aligned} \max_{\{P_i\}} \quad & \sum_{i=i_{ee}+1}^N L_i R(P_i) \\ \text{s.t.} \quad & P_i > 0, \quad i = i_{ee} + 1, \dots, N \\ & \sum_{j=i_{ee}+1}^i L_j P_j \leq \sum_{j=i_{ee}}^{i-1} E_j - \sum_{j=i_{ee}+1}^i L_j \alpha, \\ & \quad i = i_{ee} + 1, \dots, N. \end{aligned} \quad (18)$$

The optimal solution for the above problem has been shown in [12], [13] to follow a non-decreasing piecewise-constant (staircase) function, which is given in (16). It is worth noting that the staircase power allocation achieves the maximum SE for an equivalent AWGN channel subject to a sequence of energy harvesting power constraints

(modified to take into account the circuit power α) for $i = i_{ee} + 1, \dots, N$.

From the above discussion, it is revealed that for the throughput maximization in an energy harvesting transmission system subject to the non-ideal circuit power, the optimal transmission unifies both the EE and SE maximization policies independently developed in [7] and [12], [13], respectively. To summarize, one algorithm for solving the problem in (6) for the general case of $N \geq 1$ is given in Table I.

TABLE I
OPTIMAL OFF-LINE POLICY FOR SINGLE-CHANNEL CASE

Algorithm
<p>1) Calculate P_{ee} and obtain i_{ee} as</p> $i_{ee,0} = 0,$ $i_{ee,j} = \min \left\{ i \left \frac{\sum_{k=i_{ee,j-1}}^{i-1} E_k}{\sum_{k=i_{ee,j-1}+1}^i L_k} - \alpha \leq P_{ee}, \right. \right.$ $\left. i = i_{ee,j-1} + 1, \dots, N \right\}, j \geq 1,$ $J = \arg \max_{j \geq 0} i_{ee,j}, \quad i_{ee} = i_{ee,J}.$ <p>2) For the first i_{ee} epochs, set</p> $P_i^* = P_{ee}, i = 1, \dots, i_{ee},$ $l_1^{\text{on}*} = \min \left(\frac{E_0}{P_{ee} + \alpha}, L_1 \right)$ $l_i^{\text{on}*} = \min \left(\frac{\sum_{j=1}^{i-1} E_j}{P_{ee} + \alpha} - \sum_{j=1}^{i-1} l_j^{\text{on}*}, L_i \right), i = 2, \dots, i_{ee}.$ <p>3) If $i_{ee} = N$, algorithm ends; otherwise, set</p> $l_i^{\text{on}*} = L_i, i = i_{ee} + 1, \dots, N.$ <p>4) Reset</p> $E'_0 \leftarrow 0, T' \leftarrow T - \sum_{j=1}^{i_{ee}} L_j, N' \leftarrow N - i_{ee},$ $L'_j \leftarrow L_{j+i_{ee}}, E'_j \leftarrow E_{j+i_{ee}}, j = 1, \dots, N'.$ <p>5) Determine</p> $i_{\min} = \arg \min_j \left\{ \frac{\sum_{k=0}^{j-1} E'_k}{\sum_{k=0}^j L'_k} - \alpha \right\}$ $P_t = \left\{ \frac{\sum_{k=0}^{i_{\min}-1} E'_k}{\sum_{k=0}^{i_{\min}} L'_k} - \alpha \right\},$ <p>and set transmit power as P_t in the next i_{\min} epochs.</p> <p>6) If $i_{\min} = N'$, algorithm ends; otherwise, reset the parameters as follows, and go to 5).</p> $E'_0 \leftarrow 0, T' \leftarrow T' - \sum_{j=1}^{i_{\min}} L'_j, N' \leftarrow N' - i_{\min},$ $L'_j \leftarrow L'_{j+i_{\min}}, E'_j \leftarrow E'_{j+i_{\min}}, j = 1, \dots, N'.$

Remark 3.1: We discuss some implementation issues on energy harvesting communication systems with the optimal transmit power allocation given in Theorem 3.1. It is worth noting that in practical wireless systems, the duration of a communication block is usually on the order of millisecond, while the energy harvesting process evolves at a much slower speed, e.g., solar and wind power typically remains constant over windows of seconds. As a result, each epoch between any two consecutive energy arrivals in our model (during which

the optimal power policy in Theorem 3.1 allocates a constant power) can be assumed to be sufficiently long, thus containing many communication blocks. In each communication block, pilot signals can be transmitted to help estimate the signal power at the receiver, which may change from one epoch to another due to transmit power adaptation; thus, the transmission rate in (2) is practically achievable with AMC at the transmitter and coherent detection at the receiver.

Example 3.1: To illustrate the optimal two-phase transmission given in Theorem 3.1, we consider an example of a band-limited AWGN channel with bandwidth $W = 1\text{MHz}$ and the noise power spectral density $N_0 = 10^{-16}\text{Watts-per-Hz (W/Hz)}$. We assume that the attenuation power loss from the transmitter to the receiver is $h = -80\text{dB}$. Considering the channel capacity with $\Gamma = 1$, we thus have $R(P) = W \log_2(1 + \frac{Ph}{\Gamma N_0 W}) = \log_2(1 + 100P)\text{Mbps}$. It is assumed that the energy arrives at time instants $[0, 4, 6, 11, 14, 16, 18]\text{sec}$, and the corresponding energy values are $[0.5, 0.5, 0.5, 1, 0.5, 0.75, 0.5]\text{Joule}$, as shown in Fig.2. It is also assumed that $T = 20\text{secs}$ and the circuit power is $\alpha = 115.9\text{mW}$. Under this setup, we compute $P_{ee} = 79.2\text{mW}$. In Fig. 2, we compare the optimal allocation of the total consumed transmitter power by the algorithm in Table I with that obtained by the algorithm given in [12], [13]. Note that the algorithm in [12] or [13] solves (6) in the special case with the ideal circuit power $\alpha = 0$. Here, we apply this algorithm to obtain a suboptimal power allocation with $\alpha > 0$, by assuming that the transmitter is always on, i.e., $l_i^{\text{on}} = L_i, i = 1, \dots, N$. As observed in Fig. 2(a), the optimal power allocation has a two-phase structure, i.e., an on-off transmission with transmit power P_{ee} when $0 < t \leq t_3$ followed by a continuous transmission with non-decreasing staircase power allocation when $t_3 < t \leq T$, which is in accordance with Theorem 3.1. In contrast, as observed in Fig. 2(b), the suboptimal power allocation by the algorithm in [12] or [13] with the transmitter always on results in a continuous transmission with non-decreasing staircase power allocation during the entire block i.e. $0 < t \leq T$. In addition, it can be shown that the proposed optimal solution achieves the total throughput 63.14Mbps, while the suboptimal solution achieves only 55.80Mbps, over $T = 20\text{secs}$.

IV. MULTI-CHANNEL OPTIMIZATION

In this section, we extend the optimal off-line power allocation for the single-channel case to the general case with multiple parallel AWGN channels subject to a total energy harvesting power constraint and the non-ideal circuit power consumption at the transmitter. The multi-channel setup is applicable when the communication channel is decomposable into orthogonal channels by joint transmitter and receiver signal processing such as OFDM (orthogonal frequency division multiplexing) and/or MIMO (multiple-input multiple-output).

Without loss of generality, we assume a power vector $\mathbf{Q}(t) = [Q_1(t), \dots, Q_K(t)] \geq 0, t \in (0, T]$, with each element denoting the power allocation over time in one of a total K parallel AWGN channels, where $\mathbf{Q}(t) \geq 0$ denotes that $\mathbf{Q}(t)$ is elementwise no smaller than zero. We also assume a sum-throughput over the K channels, denoted by $C(t) = R(\mathbf{Q}(t))$, which satisfies

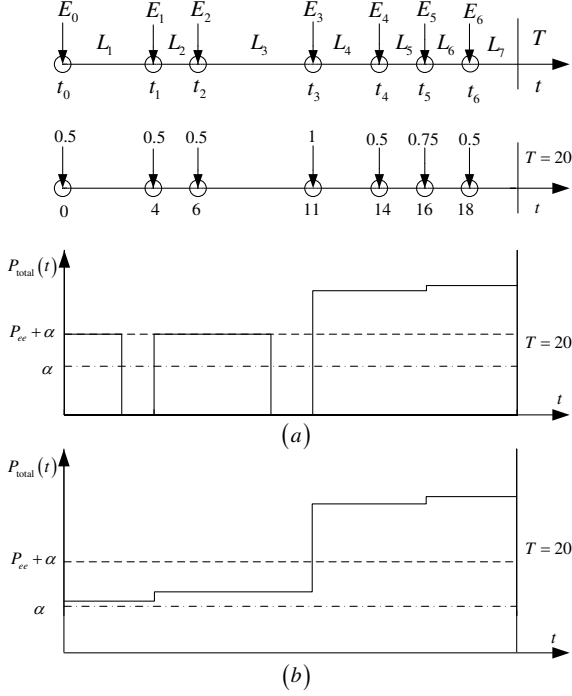


Fig. 2. Power allocation by off-line policies: (a) the optimal off-line policy; and (b) the off-line policy in [12], [13].

- 1) $R(\mathbf{Q}(t)) \geq 0, \forall \mathbf{Q}(t) \succeq 0$, and $R(\mathbf{0}) = 0$;
- 2) $R(\mathbf{Q}(t))$ is a strictly joint concave function over $\mathbf{Q}(t) \succeq 0$;
- 3) $R(\mathbf{Q}(t))$ is a monotonically increasing function with respect to each argument in $\mathbf{Q}(t)$ i.e. $Q_k(t) \geq 0, k = 1, \dots, K$.

An example of the above multi-channel sum-throughput is the sum-rate over K parallel AWGN channels achieved by joint AMC, which is given by

$$R(\mathbf{Q}(t)) = W \sum_{k=1}^K \log_2 \left(1 + \frac{h_k Q_k(t)}{\Gamma W N_0} \right), \quad (19)$$

where $h_k \geq 0$ denotes the channel power gain of the k th channel. Similar to (3) in the single-channel case, by taking into account the non-ideal circuit power α , the total power consumed at the transmitter for the multi-channel case is modeled by

$$Q_{\text{total}}(t) = \begin{cases} \sum_{k=1}^K Q_k(t) + \alpha, & \sum_{k=1}^K Q_k(t) > 0 \\ 0, & \sum_{k=1}^K Q_k(t) = 0. \end{cases} \quad (20)$$

Then the throughput maximization problem over a finite horizon T in the multi-channel case is formulated as

$$\begin{aligned} \max_{\mathbf{Q}(t) \succeq 0} \quad & \int_0^T R(\mathbf{Q}(t)) dt \\ \text{s.t.} \quad & \int_0^{t_i} Q_{\text{total}}(t) dt \leq \sum_{j=0}^{i-1} E_j, \quad i = 1, \dots, N. \end{aligned} \quad (21)$$

Similar to (5), the above problem is non-convex with $\alpha > 0$ and thus cannot be solved by standard convex optimization techniques. In the following, we will apply the principle of *nested optimization* to convert this problem with multi-dimensional (vector) power optimization to an equivalent problem with only one-dimensional (scalar) power optimization, which is then optimally solvable by the algorithm in Table I for the single-channel case.

To apply the nested optimization, we first introduce an auxiliary variable $P(t) = \sum_{k=1}^K Q_k(t)$, and rewrite the objective function of (21) equivalently as

$$\begin{aligned} \max_{P(t) \geq 0} \quad & \max_{\mathbf{Q}(t): Q_k(t) \geq 0, \sum_{k=1}^K Q_k(t) \leq P(t)} \int_0^T R(\mathbf{Q}(t)) dt \\ = \max_{P(t) \geq 0} \quad & \int_0^T \max_{\mathbf{Q}(t): Q_k(t) \geq 0, \sum_{k=1}^K Q_k(t) \leq P(t)} R(\mathbf{Q}(t)) dt. \end{aligned} \quad (22)$$

Define the auxiliary function

$$\bar{R}(P(t)) = \max_{\mathbf{Q}(t): Q_k(t) \geq 0, \sum_{k=1}^K Q_k(t) \leq P(t)} R(\mathbf{Q}(t)) \quad (23)$$

for which it can be easily verified that the maximum is attained when $\sum_{k=1}^K Q_k(t) = P(t)$. Thus, without loss of generality, we can rewrite (21) equivalently as

$$\begin{aligned} \max_{P(t) \geq 0} \quad & \int_0^T \bar{R}(P(t)) dt \\ \text{s.t.} \quad & \int_0^{t_i} P_{\text{total}}(t) dt \leq \sum_{j=0}^{i-1} E_j, \quad i = 1, \dots, N \end{aligned} \quad (24)$$

where

$$P_{\text{total}}(t) = \begin{cases} P(t) + \alpha, & P(t) > 0 \\ 0, & P(t) = 0. \end{cases} \quad (25)$$

Thus, the original problem with vector power optimization is converted by the nested optimization to an equivalent problem with only scalar power optimization. Thereby, we can first solve (24) to get the optimal solution of $P(t)$, and then with the obtained $P(t)$ solve (23) to find the optimal solution of $\mathbf{Q}(t)$ for (21). Since the problem in (23) is a convex optimization problem, it can be solved by standard techniques e.g. the Lagrange duality method [17] (in the special case of the sum-rate given in (19), the optimal solution can be obtained by the well-known “water-filling” algorithm [17]).

In order to solve (24), we first give the following proposition.

Proposition 4.1: The function $\bar{R}(P(t))$ satisfies the following properties:

- 1) $\bar{R}(P(t)) \geq 0, \forall P(t) \geq 0$, and $\bar{R}(0) = 0$;
- 2) $\bar{R}(P(t))$ is a strictly concave function over $P(t) \geq 0$;
- 3) $\bar{R}(P(t))$ is a monotonically increasing function over $P(t) \geq 0$.

Proof: See Appendix D. ■

Since $\bar{R}(P(t))$ satisfies the same conditions as $R(P(t))$ for the single-channel case, it follows that (24) can be similarly

solved by the algorithm in Table I, with one minor modification: the EE-maximizing power allocation in the multi-channel case needs to be obtained as

$$P_{ee} = \arg \max_{P>0} \frac{\bar{R}(P)}{P + \alpha}$$

$$= \arg \max_{P>0} \frac{\max_{\mathbf{Q}: Q_k \geq 0, \forall k, \sum_{k=1}^K Q_k \leq P} R(\mathbf{Q})}{P + \alpha}. \quad (26)$$

Since the maximum in the above problem is attained by $\sum_{k=1}^K Q_k = P$, the optimal solution of \mathbf{Q} is obtained as

$$\mathbf{Q}^{ee} = \arg \max_{\mathbf{Q}: Q_k \geq 0, \forall k, \sum_{k=1}^K Q_k \leq P} \frac{R(\mathbf{Q})}{\sum_{k=1}^K Q_k + \alpha} \quad (27)$$

with $\mathbf{Q}^{ee} = [Q_1^{ee}, \dots, Q_K^{ee}]$, and

$$P_{ee} = \sum_{k=1}^K Q_k^{ee}. \quad (28)$$

Since the RHS of (27) is a quasi-concave function, this problem is quasi-convex and thus can be efficiently solved by the bisection method [17]. Here we omit the detail for brevity.

To summarize, the algorithm for solving (21) for the multi-channel case is given in Table II.

TABLE II
OPTIMAL OFF-LINE POLICY FOR MULTI-CHANNEL CASE

Algorithm
1) Obtain P_{ee} by solving (27) and (28); apply the algorithm in Table I to obtain the solution $P^*(t)$ for (24).
2) With the obtained $P^*(t)$, solve (23) to obtain the solution $\mathbf{Q}^*(t)$ for (21).

V. ONLINE ALGORITHM

In the previous two sections, we have studied the optimal off-line policies assuming the non-causal ESI at the transmitter, which provide the throughput upper bound for all online policies. In this section, we will address the practical online case with only the causal (past and present) ESI assumed to be known at the transmitter. In particular, we will propose an online policy based on the structure of the optimal off-line policy obtained previously in Section III. Due to the space limitation, we will only consider the single-channel case for the study of online algorithms, while similar results can be obtained for the general multi-channel case, based on the optimal off-line policy given in Section IV.

A. Proposed Online Algorithm

For the purpose of exposition, we assume that the harvested energy is modeled by a compound Poisson process, where the number of energy arrivals over a horizon T follows a Poisson distribution with mean $\lambda_e T$ and the energy amount in each arrival is independent and identically (i.i.d.) distributed with mean \bar{E} . It is assumed that λ_e and \bar{E} are known at the transmitter.

We propose an online power allocation algorithm based on the structure of the optimal off-line solution revealed in Theorem 3.1. Specifically, considering the start time of each block, from Theorem 3.1, we obtain the closed-form solution for the optimal off-line power allocation at $t = 0$ in the following proposition.

Proposition 5.1: Suppose there are $N - 1$ energy arrivals in $(0, T)$ with $N \geq 1$, the optimal off-line power allocation solution for (6) at $t = 0$ is given by

$$P^*(0) = \max \left(\min_{i=1, \dots, N} \left(\frac{\sum_{k=0}^{i-1} E_k}{\sum_{k=1}^i L_k} - \alpha \right), P_{ee} \right). \quad (29)$$

Proof: See Appendix E. ■

Note that in (29), E_0 is available at the transmitter at $t = 0$, while N , E_i , $i = 1, \dots, N - 1$, and L_i , $i = 1, \dots, N$, are all unknown at the transmitter due to the causal ESI. As a result, we cannot compute $P^*(0)$ in (29) at $t = 0$ for the online policy. Nevertheless, we can approximate the expression of $P^*(0)$ based on the statistical knowledge of the energy arrival process, i.e., λ_e and \bar{E} , as follows.

Denote

$$\frac{\sum_{k=0}^{i-1} E_k}{\sum_{k=1}^i L_k} = \frac{E_0 + \sum_{k=1}^{i-1} E_k}{\sum_{k=1}^i L_k} = \frac{E_0}{\sum_{k=1}^i L_k} + \frac{\sum_{k=1}^{i-1} E_k}{\sum_{k=1}^i L_k}.$$

For any $i \leq N$, $\sum_{k=1}^{i-1} E_k$ is the total energy harvested during $(0, t_i)$ and $\sum_{k=1}^i L_k = t_i$. We thus have

$$\frac{\sum_{k=1}^{i-1} E_k}{\sum_{k=1}^i L_k} \approx \frac{\lambda_e t_i \bar{E}}{t_i} = \lambda_e \bar{E}, \quad \forall 1 < i \leq N, \quad (30)$$

where the approximation becomes exact when $t_i \rightarrow \infty$.

Using (30), we can approximate $\frac{\sum_{k=0}^{i-1} E_k}{\sum_{k=1}^i L_k}$ as $\frac{E_0}{\sum_{k=1}^i L_k} + \lambda_e \bar{E}$, and

$$\min_{i=1, \dots, N} \left(\frac{\sum_{k=0}^{i-1} E_k}{\sum_{k=1}^i L_k} - \alpha \right) \approx \min_{i=1, \dots, N} \left(\frac{E_0}{\sum_{k=1}^i L_k} + \lambda_e \bar{E} - \alpha \right) = \frac{E_0}{T} + \lambda_e \bar{E} - \alpha,$$

and then obtain

$$P^*(0) \approx \max \left(\frac{E_0}{T} + \lambda_e \bar{E} - \alpha, P_{ee} \right). \quad (31)$$

Since E_0 , λ_e and \bar{E} are all known at the transmitter at $t = 0$, (31) can be computed in real time.

For any $0 < t < T$, by denoting the stored energy as $E_s(t)$ with $E_s(0) = E_0$, we can view the online throughput maximization at time t over the remaining time $T - t$ to have an initial stored energy $E_0 = E_s(t)$. Therefore, by replacing T and E_0 in (31) as $T - t$ and $E_s(t)$, respectively, we obtain the following online transmit power allocation policy:

$$P_{\text{online}}(t) = \begin{cases} \max \left(\frac{E_s(t)}{T-t} + \lambda_e \bar{E} - \alpha, P_{ee} \right), & E_s(t) > 0 \\ 0, & E_s(t) = 0 \end{cases} \quad (32)$$

for any $t \in [0, T)$.

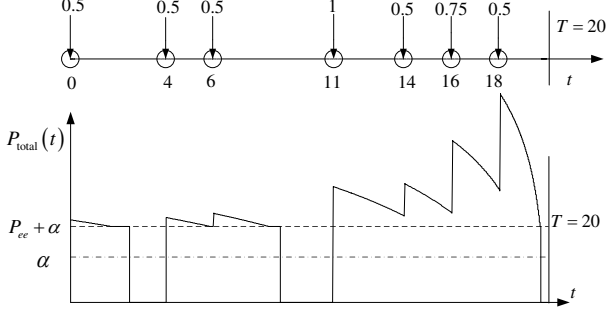


Fig. 3. Power allocation by the proposed online policy.

The online policy in (32) provides some useful insights. Note that $\frac{E_s(t)}{T-t} + \lambda_e \bar{E} - \alpha$ can be viewed as the “expected” available transmit power for the remaining time in each block, which can be negative for some t if $\frac{E_s(t)}{T-t} + \lambda_e \bar{E} < \alpha$. Thus, if this value is less than the EE-maximizing power allocation P_{ee} , the transmitter should transmit with P_{ee} to save energy; however, if the inequality is reversed, the transmitter should transmit more power to maximize the SE. Moreover, as compared to the optimal off-line power allocation for the single-epoch case given in Proposition 3.1, we see that the online policy (32) bears a similar structure, by noting that $E_0/T - \alpha$ in (8) for the single-epoch case is also the available transmit power for the remaining time in each block. Last, it is worth remarking that the online power allocation policy in (32) is expressed as a function of the continuous time for convenience; however, in practice, this policy needs to be implemented in discrete time steps by properly quantizing the continuous-time function. The time step needs to be carefully chosen in implementation: On one hand, it is desirable to use smaller step values to achieve higher quantization accuracy for energy saving, while on the other hand, the time step needs to be sufficiently large, i.e., at least larger than one communication block (cf. Remark 3.1) so that the receiver can have a timely estimate of any transmit power adjustment.

Example 5.1: To illustrate the proposed online power allocation policy in (32), we consider the same channel setup and harvested energy process for the off-line case in Example 3.1 (cf. Fig. 2). In Fig. 3, we show the total transmitter power consumption by the proposed online policy assuming that the exact average harvested power $\lambda_e \bar{E} = (\sum_{i=1}^{N-1} E_i)/T = 187.5\text{mW}$ is known at the transmitter. It is observed that the online power allocation is no more piecewise-constant like the optimal off-line power allocation in Fig. 2(a). Nevertheless, it is also observed that these two policies result in some similar power allocation patterns, i.e., starting with an on-off power allocation followed by a non-decreasing (in the sense of average power profile for the online policy case) power allocation. This suggests that the proposed online policy captures the essential features of the optimal off-line policy. Moreover, it can be shown that the proposed online policy achieves the total throughput 61.61Mbits over $T = 20\text{secs}$, which is only 1.53Mbits from 63.14Mbits of the optimal off-line policy. In addition, it can be verified that the total

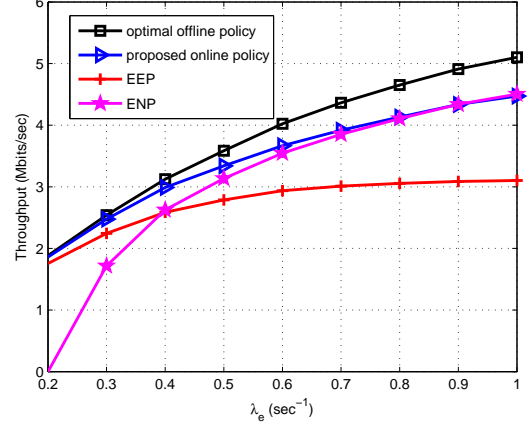


Fig. 4. Average throughput versus the energy arrival rate λ_e with $\bar{E} = 0.5\text{J}$ and $T = 20\text{secs}$.

throughput obtained by the proposed online policy is very robust to the assumed average harvested power value $\lambda_e \bar{E}$. For example, by setting $\lambda_e \bar{E}$ to be 150mW or 200mW, the proposed online policy obtains the throughput 61.38Mbits and 61.60Mbits, respectively, which is a very small loss in either case.

VI. SIMULATION RESULTS

In the section, we compare the performance of the proposed online policy with the performance upper bound achieved by the optimal off-line policy under a stochastic energy harvesting setup modeled by the compound Poisson process. The amount of energy in each energy arrival is assumed to be independent and uniformly distributed between 0 and $2\bar{E}$. For the purpose of comparison, we also consider two alternative heuristically designed online power allocation policies given as follows.

- **Energy Efficient Policy (EEP):** In this online policy, the transmitter transmits with the EE-maximizing power allocation P_{ee} given in (10) provided that there is a non-zero stored energy, i.e.,

$$P_{\text{EEP}}(t) = \begin{cases} P_{ee}, & E_s(t) > 0 \\ 0, & E_s(t) = 0 \end{cases} \quad (33)$$

for any $t \in [0, T)$.

- **Energy Neutralization Policy (ENP):** This online policy transmits with a constant power that satisfies the long-term energy consumption constraint if there is available stored energy, i.e.,

$$P_{\text{ENP}}(t) = \begin{cases} \lambda_e \bar{E} - \alpha, & E_s(t) > 0 \\ 0, & E_s(t) = 0 \end{cases} \quad (34)$$

for any $t \in [0, T)$. Note that in the above we have assumed that $\lambda_e \bar{E} > \alpha$.

First, we consider a single AWGN channel in Figs. 4 and 5 with the same channel parameters as for Example 3.1. In Fig. 4, we show the average throughput over $T = 20\text{secs}$ versus λ_e , with $\bar{E} = 0.5\text{Joule (J)}$. It is observed that when λ_e is small, the proposed online policy and EEP obtain similar performance as the optimal off-line policy. Since the average

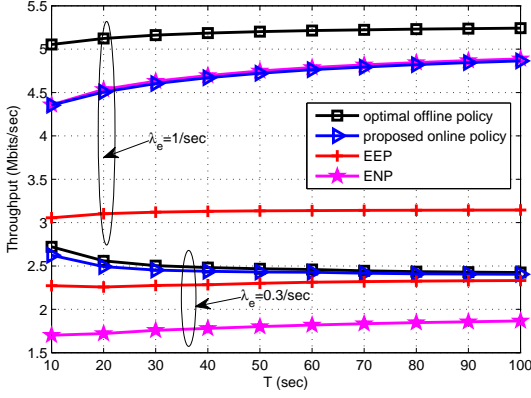


Fig. 5. Average throughput versus the block duration T with $\bar{E} = 0.5J$.

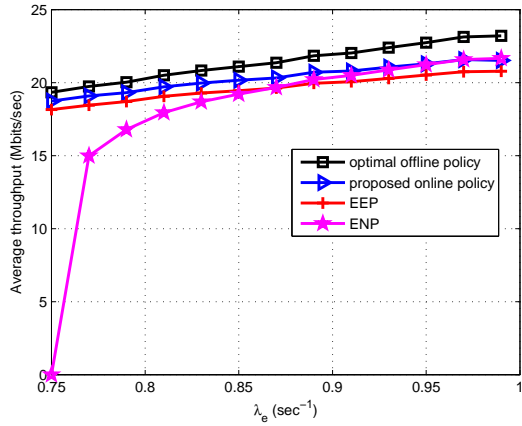


Fig. 6. Average throughput in a single-cell OFDMA downlink system with renewable powered BS versus the energy arrival rate λ_e with $\bar{E} = 200J$ and $T = 20$ secs.

harvested energy is small when λ_e is small, it is more likely that P_{ee} is greater than both $\frac{E_s(t)}{T-t} + \lambda_e E - \alpha$ (c.f. (32)) and $\sum_{k=1}^{i-1} \frac{E_k}{L_k} - \alpha, \forall i = 1, \dots, N$ (c.f. (29)). Thus, both the proposed online and off-line policies choose to transmit with P_{ee} during the “on” periods to save energy. However, for ENP, the transmit power level deviates from P_{ee} and thus significant amount of energy is consumed due to the non-ideal circuit power; as a result, the achievable throughput is almost zero. As λ_e increases, the throughput gap between the optimal off-line policy and all online policies enlarges, and the performance of EEP degenerates severely. Moreover, ENP is observed to obtain a similar performance as the proposed online policy. This is because in this case, $\frac{E_s(t)}{T-t}$ is negligibly small as compared with $\lambda_e E$, and as a result the proposed online policy degenerates to ENP.

Fig. 5 shows the average throughput versus T , for two different values of $\lambda_e = 0.3/\text{sec}$ and $1/\text{sec}$, with $\bar{E} = 0.5J$. In both cases of λ_e , the proposed online policy is observed to perform close to the optimal off-line policy, for all values of T . With small value of λ_e , i.e., $\lambda_e = 0.3/\text{sec}$, EEP performs much better than ENP since it is more energy efficient, while with a larger value of λ_e , i.e., $\lambda_e = 1/\text{sec}$, the reverse becomes

true, which can be similarly explained as for Fig. 4.

Furthermore, for the multi-channel scenario, in Fig. 6 we evaluate the average throughput of a single-cell downlink system with the base station (BS) powered by energy harvesting. It is assumed that the BS covers a circular area with radius 1000 meters, and serves K users whose locations are generated following a spatial homogeneous Poisson point process (HPPP) with density 10^{-6} users/m². Consider a simplified channel model without fading, in which the channel power gain of each user from the BS is determined by a pathloss model $c_0 \left(\frac{r}{r_0}\right)^{-\zeta}$, where $c_0 = -60\text{dB}$ is a constant equal to the pathloss at a reference distance $d_0 = 10\text{m}$, and $\zeta = 3$ is the pathloss exponent. Assuming an OFDMA (orthogonal frequency division multiplexing access) based user multiple access, a total bandwidth $W = 5\text{MHz}$ is equally allocated to the K users. The noise power spectral density at each user receiver is set as $N_0 = -174\text{dBm/Hz}$ and $\Gamma = 1$ is assumed. The circuit power at the BS is set as $\alpha = 60\text{Watt}$. Fig. 6 shows the average throughput versus λ_e with $\bar{E} = 200J$ and an energy scheduling period $T = 20\text{secs}$. It is observed that the proposed online policy always performs better than EEP. With small values of λ_e , i.e., $\lambda_e \leq 0.8/\text{sec}$, ENP performs clearly worse than the proposed online algorithm, while when $\lambda_e \geq 0.95/\text{sec}$, both schemes perform similarly. This observation is expected as can be similarly explained for Fig. 4.

VII. CONCLUDING REMARKS

In this paper, we studied the throughput-optimal transmission policies for energy harvesting wireless transmitters with the non-ideal circuit power. We first obtained the optimal off-line solution in the single-channel case, which is shown to have a new two-phase transmission structure by unifying existing results on separately maximizing energy efficiency and spectrum efficiency. We then extended the optimal off-line solution to the general case with multiple AWGN channels subject to a total energy harvesting power constraint, by the technique of nested optimization. Finally, we proposed an online algorithm based on a closed-form off-line solution. It is shown by simulations that the proposed online algorithm has a very close performance to the upper bound achieved by the optimal off-line solution, and also outperforms other heuristically designed online algorithms.

After submission of this manuscript, we become aware of one interesting related work [19] that is worth mentioning. In [19], the throughput optimization in a single-channel energy harvesting communication system with battery leakage is introduced. The impact of battery leakage is very similar to that of the non-ideal circuit power considered in this paper; as a result, the optimal transmission policy developed in [19] is similar to the one proposed in Section III of this paper. One difference is that the optimal off-line policy in [19] is developed by decoupling the general multi-epoch problem into multiple equivalent single-epoch subproblems, while the same optimal policy in this paper is derived by decoupling the problem into only two subproblems (c.f. Appendix C). Compared with the solution in [19], the off-line policy in this paper reveals the optimal two-phase structure in which EE and

SE optimizations are unified, and thus motivates our online policies, which are not given in [19].

APPENDIX A PROOF OF LEMMA 3.1

Denote the length of the on-period $\mathcal{T}_i^{\text{on}}$ as l_i^{on} and that of the off-period $\mathcal{T}_i^{\text{off}}$ as l_i^{off} , where $l_i^{\text{on}} + l_i^{\text{off}} = L_i$. Without loss of generality, we only need to consider the case with on-period $\mathcal{T}_i^{\text{on}} = (t_{i-1}, t_{i-1} + l_i^{\text{on}}]$ and off-period $\mathcal{T}_i^{\text{off}} = (t_{i-1} + l_i^{\text{on}}, t_i]$, since exchanging the power allocation at two different time instants in an epoch does not change the throughput and the energy constraint. Next, we prove that the transmit power should be constant during the on-period $\mathcal{T}_i^{\text{on}}$ in an epoch by contradiction.

Suppose that the optimal allocated transmit power $\bar{P}(t)$, where $\bar{P}(t) > 0, t \in (t_{i-1}, t_{i-1} + l_i^{\text{on}}]$ is not constant. Since $R(P(t))$ is a strictly concave function, based on Jensen's inequality, we have

$$R\left(\frac{\int_{t_{i-1}}^{t_{i-1}+l_i^{\text{on}}} \bar{P}(t)dt}{l_i^{\text{on}}}\right) > \int_{t_{i-1}}^{t_{i-1}+l_i^{\text{on}}} \frac{R(\bar{P}(t))}{l_i^{\text{on}}} dt, \quad (35)$$

and then

$$\begin{aligned} & \int_{t_{i-1}}^{t_{i-1}+l_i^{\text{on}}} R\left(\frac{\int_{t_{i-1}}^{t_{i-1}+l_i^{\text{on}}} \bar{P}(t)dt}{l_i^{\text{on}}}\right) dt \\ &= l_i^{\text{on}} R\left(\frac{\int_{t_{i-1}}^{t_{i-1}+l_i^{\text{on}}} \bar{P}(t)dt}{l_i^{\text{on}}}\right) \\ &> \int_{t_{i-1}}^{t_{i-1}+l_i^{\text{on}}} R(\bar{P}(t)) dt. \end{aligned} \quad (36)$$

Thus, if we construct a new transmit power allocation $\hat{P}(t)$ as $\hat{P}(t) = P_i = \frac{\int_{t_{i-1}}^{t_{i-1}+l_i^{\text{on}}} \bar{P}(t)dt}{l_i^{\text{on}}} > 0, t \in (t_{i-1}, t_{i-1} + l_i^{\text{on}}]$, we can achieve a larger throughput than that achieved by $\bar{P}(t)$. Moreover, we verify that $\hat{P}(t)$ consumes the same total energy as $\bar{P}(t)$ in the i th epoch, i.e.,

$$\begin{aligned} & \int_{t_{i-1}}^{t_{i-1}+l_i^{\text{on}}} (\hat{P}(t) + \alpha) dt = l_i^{\text{on}}(P_i + \alpha) \\ &= \int_{t_{i-1}}^{t_{i-1}+l_i^{\text{on}}} \bar{P}(t) dt + l_i^{\text{on}}\alpha = \int_{t_{i-1}}^{t_{i-1}+l_i^{\text{on}}} (\bar{P}(t) + \alpha) dt. \end{aligned} \quad (37)$$

Therefore, based on (36) and (37), we conclude that $\bar{P}(t)$ cannot be optimal and thus Lemma 3.1 is proved.

APPENDIX B PROOF OF PROPOSITION 3.1

To solve (7), we note that the third inequality constraint must be met with equality by the optimal solution, since otherwise the throughput can be further improved by increasing P_1 . Thus, by substituting $l_1^{\text{on}} = \frac{E_0}{P_1 + \alpha}$ into the objective function

as well as the constraint $l_1^{\text{on}} \leq T$, the problem becomes equivalent to finding

$$\begin{aligned} P_1^* &= \arg \max_{P_1 > 0, P_1 \geq E_0/T - \alpha} \frac{E_0}{P_1 + \alpha} R(P_1) \\ &= \arg \max_{P_1 > 0, P_1 \geq E_0/T - \alpha} \frac{R(P_1)}{P_1 + \alpha}. \end{aligned} \quad (38)$$

Consider first the following problem with the relaxed power constraint:

$$\max_{P_1 > 0} \frac{R(P_1)}{P_1 + \alpha}. \quad (39)$$

This problem has been studied in [7], where the globally optimal solution is known as the EE-maximizing power allocation, denoted by P_{ee} . It was also shown in [7] that given $\alpha > 0$, $\frac{R(P_1)}{P_1 + \alpha}$ is monotonically increasing with P_1 if $0 \leq P_1 < P_{ee}$, and monotonically decreasing with P_1 if $P_1 > P_{ee}$. Thus, the solution of (38) is obtained as

$$P_1^* = \max\left(P_{ee}, \frac{E_0}{T} - \alpha\right). \quad (40)$$

Accordingly, the optimal on-period is given by

$$l_1^{\text{on}*} = \frac{E_0}{P_1^* + \alpha}. \quad (41)$$

Proposition 3.1 is thus proved.

APPENDIX C PROOF OF THEOREM 3.1

To prove Theorem 3.1, we construct the following two sub-problems \mathbb{P}_1 and \mathbb{P}_2 for the power allocation optimization in the first i_{ee} epochs and the last $N - i_{ee}$ epochs, respectively.

$$\begin{aligned} \mathbb{P}_1 : & \max_{\{P_i\}, \{l_i^{\text{on}}\}} \sum_{i=1}^{i_{ee}} l_i^{\text{on}} R(P_i), \\ & \text{s.t. } 0 \leq l_i^{\text{on}} \leq L_i, i = 1, \dots, i_{ee}, \\ & \sum_{j=1}^i (P_j + \alpha) l_j^{\text{on}} \leq \sum_{j=0}^{i-1} E_j, i = 1, \dots, i_{ee}. \end{aligned} \quad (42)$$

$$\begin{aligned} \mathbb{P}_2 : & \max_{\{P_i\}, \{l_i^{\text{on}}\}} \sum_{i=i_{ee}+1}^N l_i^{\text{on}} R(P_i), \\ & \text{s.t. } 0 \leq l_i^{\text{on}} \leq L_i, i = i_{ee} + 1, \dots, N \\ & \sum_{j=i_{ee}+1}^i (P_j + \alpha) l_j^{\text{on}} \leq \sum_{j=i_{ee}}^{i-1} E_j, \\ & i = i_{ee} + 1, \dots, N. \end{aligned} \quad (43)$$

We will first prove that the solution given in Theorem 3.1 is optimal for both \mathbb{P}_1 and \mathbb{P}_2 , and then prove that the optimal solutions for \mathbb{P}_1 and \mathbb{P}_2 are also optimal for (6).

First, we prove that the solution given in (12), (13) and (14) is optimal for \mathbb{P}_1 .

Consider the throughput maximization problem \mathbb{P}_1 , with the arrived energy $E_0, \dots, E_{i_{ee}-1}$ at time $t_0, \dots, t_{i_{ee}-1}$ over the horizon $T_1 = \sum_{k=1}^{i_{ee}} L_k$. We construct an auxiliary throughput maximization problem \mathbb{P}_1 with the energy arrival

$\sum_{k=0}^{i_{ee}-1} E_k, 0, \dots, 0$ at time $t_0, \dots, t_{i_{ee}-1}$ over the same horizon T_1 as follows.

$$\begin{aligned} \bar{\mathbb{P}}_1 : \quad & \max_{\{P_i\}, \{l_i^{\text{on}}\}} \sum_{i=1}^{i_{ee}} l_i^{\text{on}} R(P_i), \\ & \text{s.t. } 0 \leq l_i^{\text{on}} \leq L_i, i = 1, \dots, i_{ee}, \\ & \sum_{j=1}^{i_{ee}} (P_j + \alpha) l_j^{\text{on}} \leq \sum_{j=0}^{i_{ee}-1} E_j. \end{aligned} \quad (44)$$

It is clear that the optimal throughput of $\bar{\mathbb{P}}_1$ is an upper bound on that of \mathbb{P}_1 since any feasible solution of \mathbb{P}_1 is also feasible for $\bar{\mathbb{P}}_1$. Note that there is no energy arrived in $t_1, \dots, t_{i_{ee}-1}$ for $\bar{\mathbb{P}}_1$, so $\bar{\mathbb{P}}_1$ is indeed equivalent to a throughput maximization problem for the single-epoch case studied in Section III-B over a horizon T_1 . It can be easily verified based on (11) that $\frac{\sum_{j=0}^{i_{ee}-1} E_j}{T_1} - \alpha \leq P_{ee}$; thus, it follows after some simple manipulation that the optimal value of $\bar{\mathbb{P}}_1$ is $\frac{\sum_{j=0}^{i_{ee}-1} E_j}{P_{ee} + \alpha} \cdot R(P_{ee})$ and is attained by $\bar{P}_1^* = \dots = \bar{P}_{i_{ee}}^* = P_{ee}$ and $\sum_{j=1}^{i_{ee}} \bar{l}_j^{\text{on}*} = \frac{\sum_{j=0}^{i_{ee}-1} E_j}{P_{ee} + \alpha}$. Meanwhile, for \mathbb{P}_1 we can always construct a feasible solution based on (12), (13) and (14) by setting

$$\begin{aligned} P_j^* &= P_{ee}, \quad \forall j = 1, \dots, i_{ee}, \\ l_k^{\text{on}*} &= L_k, \quad \forall k \neq i_{ee}, j, \forall j = 1, \dots, J, \\ l_{i_{ee},j}^{\text{on}*} &= \frac{\sum_{k=i_{ee},j-1}^{i_{ee},j-1} E_k}{P_{ee} + \alpha} - \sum_{k=i_{ee},j-1+1}^{i_{ee},j} L_k, \quad \forall j = 1, \dots, J. \end{aligned} \quad (45)$$

It can be verified from (11) that the solution satisfying (45) is feasible for \mathbb{P}_1 , and attains an objective value of $\frac{\sum_{j=0}^{i_{ee}-1} E_j}{P_{ee} + \alpha} \cdot R(P_{ee})$, which is the same as the optimal value of $\bar{\mathbb{P}}_1$. The gap between \mathbb{P}_1 and $\bar{\mathbb{P}}_1$ is thus zero, and accordingly, the solution given in (12), (13) and (14) is optimal for \mathbb{P}_1 .

Second, we prove that the solution in (15), (16) and (17) is optimal for Problem \mathbb{P}_2 over the last $N - i_{ee}$ epochs. First, we show $l_i^{\text{on}*} = L_i, i = i_{ee} + 1, \dots, N$ by contradiction as follows. Suppose that the optimal solution $\hat{P}(t)$ contains an “off” period with $(\hat{t}^{\text{off}}, \hat{t}^{\text{off}} + \Delta \hat{t}^{\text{off}}) \subset (t_{i_{ee}}, T]$, i.e., $\hat{P}(t) = 0, t \in (\hat{t}^{\text{off}}, \hat{t}^{\text{off}} + \Delta \hat{t}^{\text{off}})$.

Due to the definition of (11), it follows immediately that

$$\frac{\sum_{k=i_{ee}}^{i-1} E_k}{\sum_{k=i_{ee}+1}^i L_k} - \alpha > P_{ee}, \quad \forall i > i_{ee} \quad (46)$$

Therefore, we can always find a time duration with $\hat{P}(t) = \hat{P}^{\text{on}} > P_{ee}, t \in (\hat{t}^{\text{on}}, \hat{t}^{\text{on}} + \Delta \hat{t}^{\text{on}}) \subset (t_{i_{ee}}, T]$, and construct a new policy $\bar{P}(t)$ with $\bar{P}(t) = \bar{P}^{\text{on}} = \frac{(\hat{P}^{\text{on}} + \alpha) \Delta \hat{t}^{\text{on}}}{\Delta \hat{t}^{\text{on}} + \delta} - \alpha, t \in (\hat{t}^{\text{on}}, \hat{t}^{\text{on}} + \Delta \hat{t}^{\text{on}}) \cup (\hat{t}^{\text{off}}, \hat{t}^{\text{off}} + \delta)$. Note that we have chosen δ to be sufficiently small so that $(\hat{t}^{\text{off}}, \hat{t}^{\text{off}} + \delta) \subseteq (\hat{t}^{\text{off}}, \hat{t}^{\text{off}} + \Delta \hat{t}^{\text{off}})$ and $\bar{P}^{\text{on}} > P_{ee}$. The energy consumed by $\bar{P}(t)$ during $(\hat{t}^{\text{on}}, \hat{t}^{\text{on}} + \Delta \hat{t}^{\text{on}}) \cup (\hat{t}^{\text{off}}, \hat{t}^{\text{off}} + \delta)$ is $\hat{E} = (\bar{P}^{\text{on}} + \alpha)(\Delta \hat{t}^{\text{on}} + \delta) =$

$(\hat{P}^{\text{on}} + \alpha) \Delta \hat{t}^{\text{on}}$, which is same as the initial policy $\hat{P}(t)$. The throughput for the newly constructed policy $\bar{P}(t)$ and initial policy $\hat{P}(t)$ during $(\hat{t}^{\text{on}}, \hat{t}^{\text{on}} + \Delta \hat{t}^{\text{on}}) \cup (\hat{t}^{\text{off}}, \hat{t}^{\text{off}} + \delta)$ are

$$B_1 = R(\bar{P}^{\text{on}})(\Delta \hat{t}^{\text{on}} + \delta) = R(\bar{P}^{\text{on}}) \frac{\hat{E}}{\bar{P}^{\text{on}} + \alpha}$$

and

$$B_2 = R(\hat{P}^{\text{on}}) \Delta \hat{t}^{\text{on}} = R(\hat{P}^{\text{on}}) \frac{\hat{E}}{\hat{P}^{\text{on}} + \alpha}$$

respectively. Since $\hat{P}^{\text{on}} > \bar{P}^{\text{on}} > P_{ee}$, and $\frac{R(x)}{x+\alpha}$ is monotonically decreasing as a function of x when $x > P_{ee}$, we conclude that $B_1 > B_2$. Therefore, the new policy achieves a higher throughput than the initial policy.

Moreover, we need to check that the new policy also satisfies the energy constraint as follows. If $\hat{t}^{\text{off}} > \hat{t}^{\text{on}} + \Delta \hat{t}^{\text{on}}$, or $(\hat{t}^{\text{on}}, \hat{t}^{\text{on}} + \Delta \hat{t}^{\text{on}})$ and $(\hat{t}^{\text{off}}, \hat{t}^{\text{off}} + \delta)$ are in the same epoch, it is evident that the energy constraint is satisfied. If we cannot find an interval $(\hat{t}^{\text{off}}, \hat{t}^{\text{off}} + \Delta \hat{t}^{\text{off}})$ latter than or in the same epoch as $(\hat{t}^{\text{on}}, \hat{t}^{\text{on}} + \Delta \hat{t}^{\text{on}})$, i.e., all the allocated power prior to \hat{t}^{off} is smaller than P_{ee} , in this case based on (46), there must be some energy left at time \hat{t}^{off} . Since we selected δ to be sufficiently small, we can still guarantee that the energy constraint is satisfied. Therefore, we prove that $l_i^{\text{on}*} = L_i, i = i_{ee} + 1, \dots, N$.

After determining $l_i^{\text{on}*} = L_i, i = i_{ee} + 1, \dots, N$, we realize that Problem \mathbb{P}_2 for the last $N - i_{ee}$ epochs has the same structure as that studied in [12], and thus [12, Theorem 1] is applicable here. After some change of notation, we can prove that the solution in (15), (16) and (17) is optimal for \mathbb{P}_2 over the last $N - i_{ee}$ epochs.

Next, we show that the optimal solutions of \mathbb{P}_1 and \mathbb{P}_2 are optimal for (6) to complete the proof for Theorem 3.1. First, we can verify by following the similar contradiction proof in the above that any energy harvested during $[0, t_{i_{ee}})$ should be used up in the first i_{ee} epochs, i.e., $\sum_{j=1}^{i_{ee}} (P_j^* + \alpha) l_j^{\text{on}*} = \sum_{j=0}^{i_{ee}-1} E_j$. Therefore, the energy constraint for (6) is equivalent to

$$\begin{aligned} \sum_{j=1}^i (P_j + \alpha) l_j^{\text{on}} &\leq \sum_{j=0}^{i-1} E_j, \quad i = 1, \dots, i_{ee} \\ \sum_{j=i_{ee}+1}^i (P_j + \alpha) l_j^{\text{on}} &\leq \sum_{j=i_{ee}}^{i-1} E_j, \quad i = i_{ee} + 1, \dots, N. \end{aligned} \quad (47)$$

Since the energy constraint is decoupled before and after $t_{i_{ee}}$, solving (6) is equivalent to optimizing P_i and l_i^{on} over $i = 1, \dots, i_{ee}$ and $i = i_{ee} + 1, \dots, N$ separately. Thus, the optimal solutions for \mathbb{P}_1 and \mathbb{P}_2 are also optimal for (6). Theorem 3.1 is thus proved.

APPENDIX D PROOF OF PROPOSITION 4.1

The first and third properties of $\bar{R}(P(t))$ can be directly verified by the first and third properties of $R(\mathbf{Q}(t))$, respectively. Thus, to complete the proof of Proposition 4.1, we only need to show the second property of $\bar{R}(P(t))$, i.e., it is a strictly

concave function of $P(t)$. Similar to [18, Appendix B], we show the proof of this result as follows.

Since $\bar{R}(P(t))$ is obtained as the optimal value of (23), which is a convex optimization problem and satisfies the Slater's condition [17]. Thus, the duality gap for this problem is zero. As a result, $\bar{R}(P(t))$ can be equivalently obtained as the optimal value of the following min-max optimization problem:

$$\bar{R}(P) = \min_{\mu \geq 0} \max_{Q_k \geq 0} R(\mathbf{Q}) - \mu \left(\sum_{k=1}^K Q_k - P \right) \quad (48)$$

$$= \min_{\mu \geq 0} R(\mathbf{Q}^{(\mu)}) - \mu \sum_{k=1}^K Q_k^{(\mu)} + \mu P \quad (49)$$

$$= R(\mathbf{Q}^{(\mu^{(P)})}) - \mu^{(P)} \sum_{k=1}^K Q_k^{(\mu^{(P)})} + \mu^{(P)} P \quad (50)$$

where we have removed t for brevity, and in (49) $\mathbf{Q}^{(\mu)} = [Q_1^{(\mu)}, \dots, Q_K^{(\mu)}]$ is the optimal solution for the maximization problem with a given μ , while in (50) $\mu^{(P)}$ is the optimal solution for the minimization problem with a given P . Since $R(\mathbf{Q}(t))$ is a strictly joint concave function, the optimal solutions in the above must be unique. Denote ω as any constant in $[0, 1]$. Let $\mu^{(P_1)}$, $\mu^{(P_2)}$ and $\mu^{(P_3)}$ be the optimal μ for $\bar{R}(P_1)$, $\bar{R}(P_2)$ and $\bar{R}(P_3)$ with $P_3 = \omega P_1 + (1 - \omega)P_2$, respectively. For $j = 1, 2$, we have

$$\bar{R}(P_j) = R(\mathbf{Q}^{(\mu^{(P_j)})}) - \mu^{(P_j)} \sum_{k=1}^K Q_k^{(\mu^{(P_j)})} + \mu^{(P_j)} P_j \quad (51)$$

$$\leq R(\mathbf{Q}^{(\mu^{(P_3)})}) - \mu^{(P_3)} \sum_{k=1}^K Q_k^{(\mu^{(P_3)})} + \mu^{(P_3)} P_j \quad (52)$$

where *strict inequality* holds for (52) if $P_j \neq P_3$ since the optimal $\mu^{(P_j)}$, $j = 1, 2$, are unique. Thus, we have

$$\omega \bar{R}(P_1) + (1 - \omega) \bar{R}(P_2) \quad (53)$$

$$\leq R(\mathbf{Q}^{(\mu^{(P_3)})}) - \mu^{(P_3)} \sum_{k=1}^K Q_k^{(\mu^{(P_3)})} + \mu^{(P_3)} P_3 \quad (54)$$

$$= \bar{R}(P_3) \quad (55)$$

$$= \bar{R}(\omega P_1 + (1 - \omega)P_2), \quad (56)$$

where *strict inequality* holds for (54) if $\omega \in (0, 1)$. Therefore, $\bar{R}(P(t))$ is a strictly concave function over $P(t) \geq 0$. The proof of Proposition 4.1 is thus completed.

APPENDIX E

PROOF OF PROPOSITION 5.1

We prove this proposition by considering the following two cases.

First, consider the case when i_{ee} exists, i.e., $i_{ee} \in \{1, \dots, N\}$. In this case, setting P_{ee} as the transmit power at time 0 is optimal according to Table I. Furthermore, we have $\frac{\sum_{k=0}^{i_{ee,1}-1} E_k}{\sum_{k=1}^{i_{ee,1}} L_k} - \alpha < P_{ee}$ based on (11), and thus

$$\min_{i=1, \dots, N} \left(\frac{\sum_{k=0}^{i-1} E_k}{\sum_{k=1}^i L_k} - \alpha \right) \leq \frac{\sum_{k=0}^{i_{ee,1}-1} E_k}{\sum_{k=1}^{i_{ee,1}} L_k} - \alpha < P_{ee}.$$

Thus, (29) is equivalent to $P^*(0) = P_{ee}$, which is the optimal solution.

Next, consider the case when i_{ee} does not exist, which implies that $\frac{\sum_{k=0}^{j-1} E_k}{\sum_{k=1}^j L_k} - \alpha > P_{ee}, \forall j = 1, \dots, N$. Thus, we have

$$\min_{i=1, \dots, N} \left(\frac{\sum_{k=0}^{i-1} E_k}{\sum_{k=1}^i L_k} - \alpha \right) > P_{ee}$$

and (29) is equivalent to $P^*(0) = \min_{i=1, \dots, N} \left(\frac{\sum_{k=0}^{i-1} E_k}{\sum_{k=1}^i L_k} - \alpha \right)$, which is the optimal solution according to Table I.

From the above two cases, (29) coincides with the optimal solution for $P^*(0)$. Thus, Proposition 5.1 is proved.

REFERENCES

- [1] T. Chen, Y. Yang, H. Zhang, H. Kim, and K. Horneman, "Network energy saving technologies for green wireless access networks," *IEEE Wireless Commun.*, vol. 18, no. 5, pp. 30-38, Oct. 2011.
- [2] C. Han *et al.*, "Green radio: Radio techniques to enable energy-efficient wireless networks," *IEEE Commun. Mag.*, vol. 49, no. 6, pp. 46-54, Jun. 2011.
- [3] Z. Niu, Y. Wu, J. Gong, and Z. Yang, "Cell zooming for cost-efficient green cellular networks," *IEEE Commun. Mag.*, vol. 48, no. 11, pp. 74-78, Nov. 2010.
- [4] Z. Hasan, H. Boostanimehr, and V. Bhargava, "Green cellular networks: A survey, some research issues and challenges," *IEEE Commun. Surveys & Tutorials*, vol. 13, no. 4, pp. 524-540, 2011.
- [5] Y. Chen, S. Zhang, S. Xu, and G. Y. Li, "Fundamental trade-offs on green wireless networks," *IEEE Commun. Mag.*, vol. 49, no. 6, pp. 30-37, Jun. 2011.
- [6] E. Uysal-Biyikoglu, B. Prabhakar, and A. Gamal, "Energy-efficient packet transmission over a wireless link," *IEEE/ACM Trans. Network.*, vol. 10, no. 4, pp. 487-499, Aug. 2002.
- [7] G. W. Miao, N. Himayat, and G. Y. Li, "Energy-efficient link adaptation in frequency-selective channels," *IEEE Trans. Commun.*, vol. 58, no. 2, pp. 545-554, Feb. 2010.
- [8] C. Isheden, Z. Chong, E. Jorswieck, and G. Fettweis, "Framework for link-level energy efficiency optimization with informed transmitter," *IEEE Trans. Wireless Commun.*, vol. 11, no. 8, pp. 2946-2957, Aug. 2012.
- [9] O. Blume, H. Eckhardt, S. Klein, E. Kuehn, and W. M. Wajda, "Energy savings in mobile networks based on adaptation to traffic statistics," *Bell Labs Tec. J.*, vol. 15, no. 2, pp. 77-94, Sep. 2010.
- [10] H. Kim and G. Veciana, "Leveraging dynamic spare capacity in wireless system to conserve mobile terminals energy," *IEEE/ACM Trans. Network.*, vol. 18, no. 3, pp. 802-815, Jun. 2010.
- [11] A. Kansal, J. Hsu, S. Zahedi, and M. B. Srivastava, "Power management in energy harvesting sensor networks," *ACM Trans. Embed. Comput. Syst.*, vol. 6, no. 4, Sep. 2007.
- [12] J. Yang and S. Ulukus, "Optimal packet scheduling in an energy harvesting communication system," *IEEE Trans. Commun.*, vol. 60, no. 1, pp. 220-230, Jan. 2012.
- [13] C. K. Ho and R. Zhang, "Optimal energy allocation for wireless communications with energy harvesting constraints," *IEEE Trans. Sig. Process.*, vol. 60, no. 9, pp. 4808-4818, Sep. 2012.
- [14] K. Tutuncuoglu and A. Yener, "Optimum transmission policies for battery limited energy harvesting nodes," *IEEE Trans. Wireless Commun.*, vol. 99, no. 2, pp. 1-10, Feb. 2012.
- [15] Q. Bai, J. Li, and J. A. Nossek, "Throughput maximizing transmission strategy of energy harvesting nodes," in *Proc. IWCLD*, Rennes, France, Nov. 2011.
- [16] A. Goldsmith, *Wireless Communications*. Cambridge, U.K.: Cambridge Univ. Press, 2005.
- [17] S. Boyd and L. Vandenberghe, *Convex Optimization*, Cambridge University Press, 2004.
- [18] R. Zhang, F. Gao, and Y.-C. Liang, "Cognitive beamforming made practical: Effective interference channel and learning-throughput tradeoff," *IEEE Trans. Commun.*, vol. 58, no. 2, pp. 706-718, Feb. 2010.
- [19] B. Devillers and D. Gunduz, "A general framework for the optimization of energy harvesting communication systems with battery imperfections," *Journal of Commun. and Netw.*, vol. 14, no. 2, pp. 130-139, Apr. 2012.